

Electronic Supplementary Material (ESI) for Dalton Transactions.
This journal is © The Royal Society of Chemistry 2016

Supplementary Information

Self-Assembly of Arene Ruthenium Acylpyrazolone Fragments to Tetranuclear Metallacycles. Molecular Structures and Solid-State ¹⁵N CPMAS NMR Correlations.

Riccardo Pettinari,^{a*} Fabio Marchetti,^b Claudio Pettinari,^a Francesca Condello,^a Brian W. Skelton,^c Allan H. White,^d Michele Remo Chierotti^e and Roberto Gobetto.^{e*}

[a] School of Pharmacy, University of Camerino, via S. Agostino 1, 62032 Camerino MC, Italy. E-mail: riccardo.pettinari@unicam.it; Tel: +39-0737-632338;

[b] School of Science and Technology, University of Camerino, via S. Agostino 1, 62032 Camerino MC, Italy;

[c] School of Chemistry and Biochemistry M310, The University of Western Australia, Crawley, WA 6009, Australia;

[d] Centre for Microscopy, Characterization and Analysis M010, The University of Western Australia, Crawley, WA 6009, Australia;

[e] Dipartimento di Chimica and NIS Centre, University of Torino, Via P. Giuria 7, 10125 Torino, Italy.

Table of content

Crystallographic appendix	2
Relevant ¹⁹ F NMR spectra	4
TGA curve	8

Crystallographic appendix

Table S1. Crystal/Refinement Data, (1), (2) and (4)

	1	4	2
formula	C ₂₂ H ₂₄ Cl ₂ N ₂ O ₂ Ru	C ₂₇ H ₃₅ ClN ₂ O ₂ Ru	{[(C ₂₂ H ₂₄ ClN ₂ O ₂ Ru)] ₄ (O ₃ SCF ₃)} (O ₃ SCF ₃) ₃ CHCl ₃ ·2H ₂ O
<i>M_r</i> (Dal)	520.4	556.1	2691.5
cryst. syst.	Triclinic	Triclinic	Monoclinic
space group	<i>P</i> $\bar{1}$ (No.2)	<i>P</i> $\bar{1}$ (No.2)	<i>C</i> 2 (No. 5)
<i>a</i> (Å)	7.5449(2)	7.8180(3)	32.1762)
<i>b</i> (Å)	12.0143(4)	11.5430(4)	11.3815(4)
<i>c</i> (Å)	12.9409(5)	14.1909(5)	15.8038(8)
α (deg)	112.841(4)	89.197(3)	
β (deg)	95.867(3)	85.167(3)	116.629(7)
γ (deg)	103.150(3)	77.653(3)	
<i>V</i> (Å ³)	1028.27(7)	1246.55(8)	5173.7(4)
<i>D_c</i> (Z)	1.68 ₁ (2)	1.48 ₂ (2)	1.72 ₈ (2)
μ_{Mo} (mm ⁻¹)	1.044	0.76	0.93
specimen (mm)	0.25,0.18,0.04	0.62,0.32,0.23	0.13,0.13,0.07
<i>T</i> _{min/max}	0.86	0.85	0.95
2 θ_{max} (°)	68.6	75	55
<i>N_t</i>	27880	46395	27740
<i>N</i> (<i>R</i> _{int})	8240 (0.035)	12528 (0.029)	11356 (0.098)
<i>N_o</i> (<i>I</i> >2 σ (<i>I</i>))	7376	11561	6488
<i>R</i> ₁ (<i>I</i> >2 σ (<i>I</i>))	0.031	0.024	0.074
<i>wR</i> ₂ (a,b) (all data)	0.072 (0.032,0.52)	0.060 (0.025,0.35)	0.135 (0.060)
<i>S</i>	1.03	1.08	0.95
$\Delta\rho$ _{max} (eÅ ⁻³)	1.07	0.68	1.49

Table S2. Selected non-hydrogen ruthenium environment geometries, **(1)**, **(2)**, **(4)**. C(0) are the ring centroids, O,N(n2,5,6) the ligating nitrogen or oxygen atoms of segments n = 1,2.

	1	4	2 (components 1; 2)
		Distances (Å)	
Ru-C(Csub6)	2.149(9) -2.201(2)	2.1624(9) -2.1798(9)	2.135(8) 2.146(11) -2.196(8) ; -2.202(10)
Ru-C(0)	1.653	1.640	1.641 ; 1.633
Ru-Cl/N	2.4120(4)	2.3968(3)	2.152(7) ; 2.137(8)
Ru-O(n5)	2.0877(11)	2.0835(7)	2.089(6) ; 2.055(6)
Ru-O(n6)	2.108(11)	2.1024(7)	2.099(6) ; 2.089(7)
O(n5)-C(n5)	1.270(2)	1.2732(11)	1.261(11); 1.232(10)
O(n6)-C(n6)	1.258(2)	1.2646(11)	1.235(10); 1.263(11)
C(n5)-C(n4)	1.424(2)	1.4278(11)	1.441(14); 1.491(15)
C(n4)-C(n6)	1.414(2)	1.4166(12)	1.401(13); 1.412(13)
		Angles (degrees)	
C(0)-Ru-O(n5)	127.3	127.0	127.8 ; 127.4
C(0)-Ru-O(n6)	128.2	126.0	127.5 ; 124.3
C(0)-Ru-Cl/N(n2)	129.1	129.9	125.9 ; 130.9
Cl/N(n2)-Ru-O(n5)	84.50(3)	85.07(2)	88.5(3) ; 86.6(3)
Cl/N(n2)-Ru-O(n6)	84.63(3)	85.28(2)	87.8(9) ; 87.2(3)
O(n5)-Ru-O(n6)	88.25(4)	89.23(3)	86.0(2) ; 86.1(3)
Ru-O(n5)-C(n5)	123.07(10)	121.37(6)	123.4(6) ; 127.9(7)
Ru-O(n6)-C(n6)	129.13(10)	129.43(6)	132.7(6) ; 132.0(6)
Ru-N(n2)-N(n1)	-	-	122.5(6) ; 127.7(5)
Ru-N(n2)-C(n3)	-	-	135.1(6) ; 132.8(7)
N(n2)-N(n1)-C(n5)	111.85(14)	112.20(3)	114.0(8) ; 112.0(7)
N(n1)-N(n2)-C(n3)	106.05(11)	105.83(8)	102.4(8) ; 104.4(8)

Crystallographic data for the structures reported in this paper have been deposited with the Cambridge Crystallographic Data Centre as a supplementary publication no. CCDC: 945237(**1**); 945230 (**2**); 945238 (**4**). Copies of the data can be obtained free of charge on application to CCDC, 12 Union Road, Cambridge CB21EZ, UK (fax: +(44)1223-336-033; email: deposit@ccdc.cam.ac.uk).

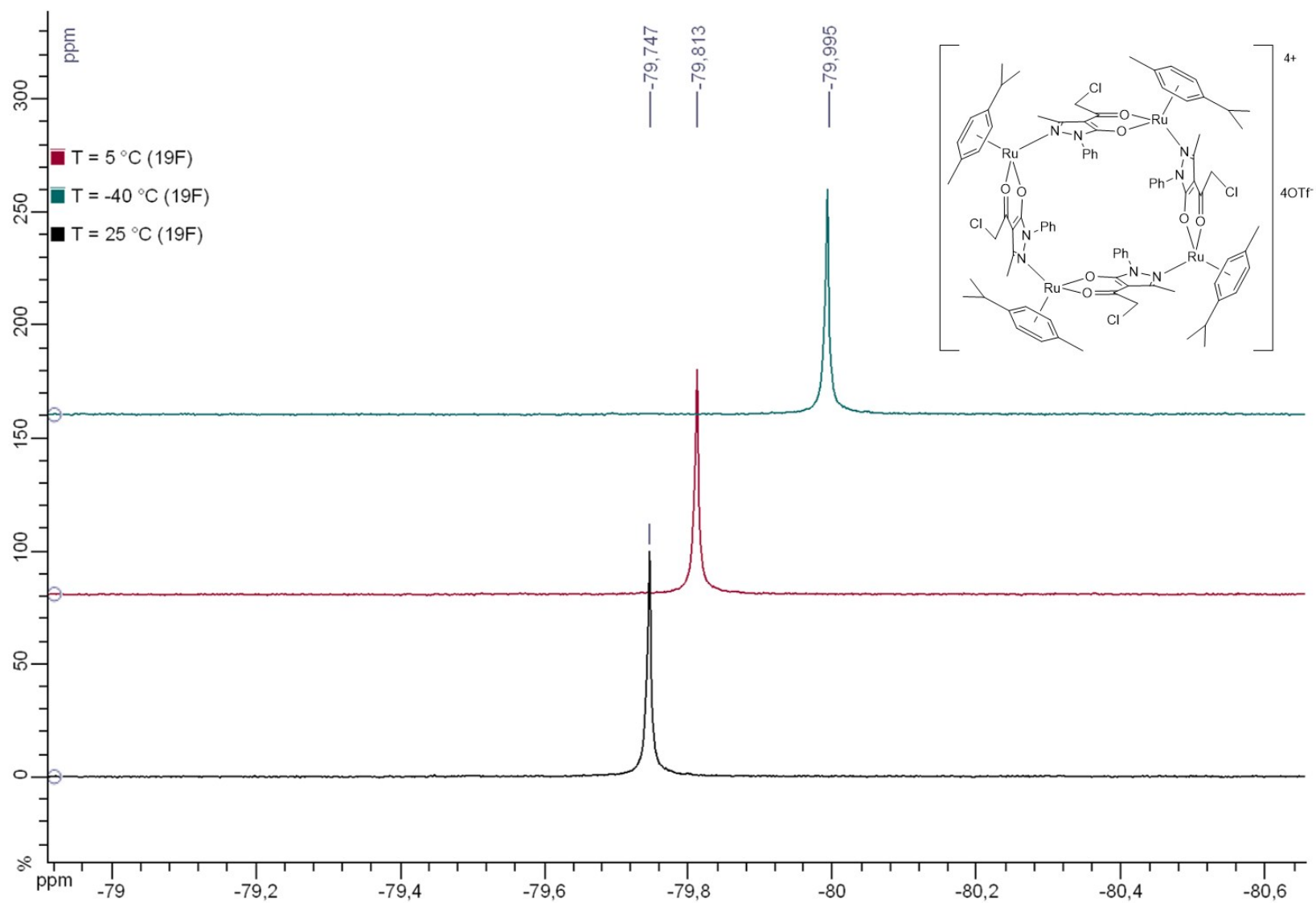


Figure S1. Variable temperature ^{19}F NMR spectra of $[(\eta^6\text{-cym})\text{Ru}(\text{Q}^{\text{CH}_2\text{Cl}})]_4(\text{SO}_3\text{CF}_3)_4$ (**4**) carried out in CD_3CN .

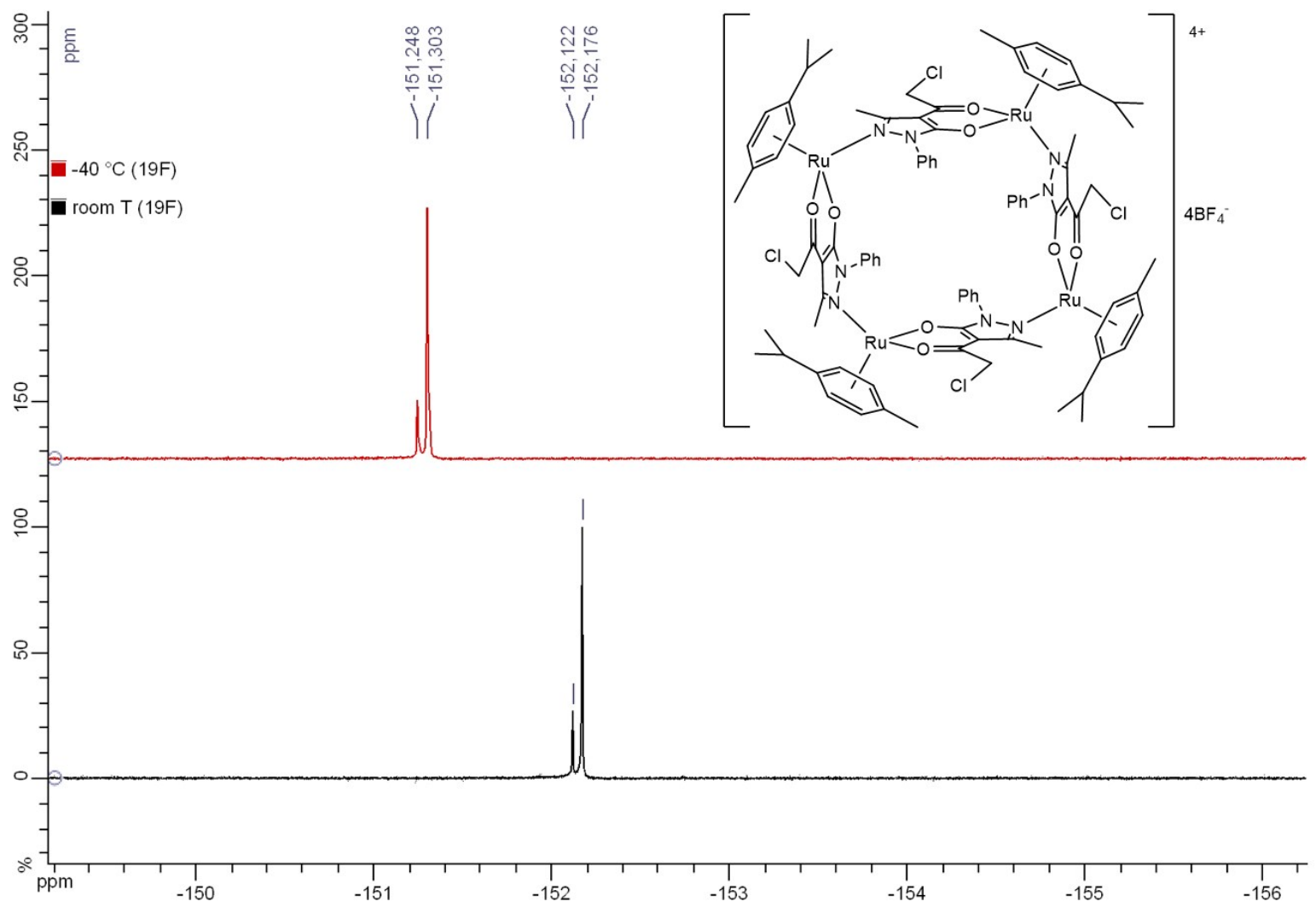


Figure S2. Variable temperature ^{19}F NMR spectra of $[(\eta^6\text{-cym})\text{Ru}(\text{Q}^{\text{CH}_2\text{Cl}})]_4(\text{BF}_4)_4$ (**5**) carried out in CD_3CN .

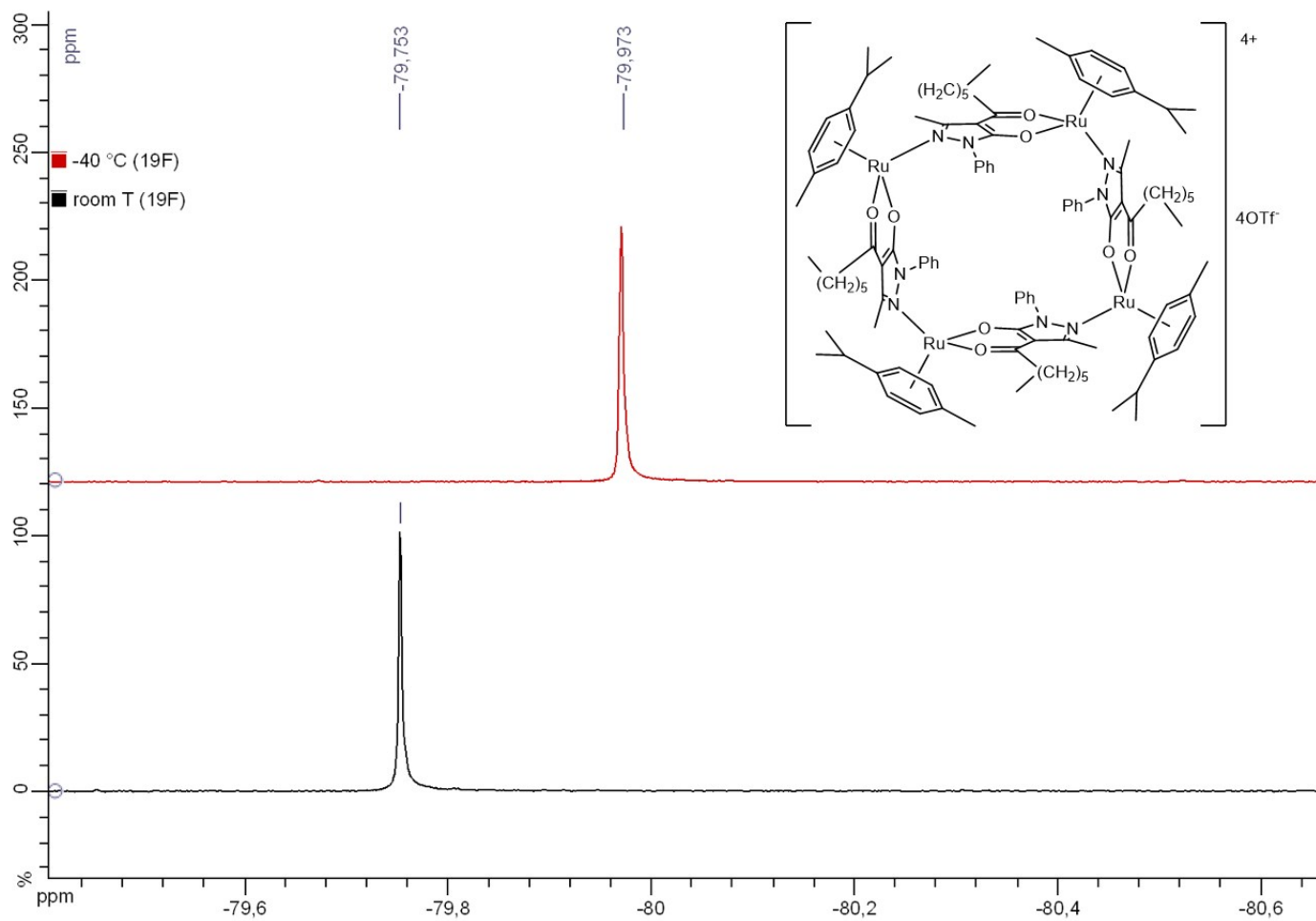


Figure S3. Variable temperature ^{19}F NMR spectra of $[(\eta^6\text{-cym})\text{Ru}(\text{Q}^{\text{hex}})]_4(\text{SO}_3\text{CF}_3)_4$ (**6**) carried out in CD_3CN .

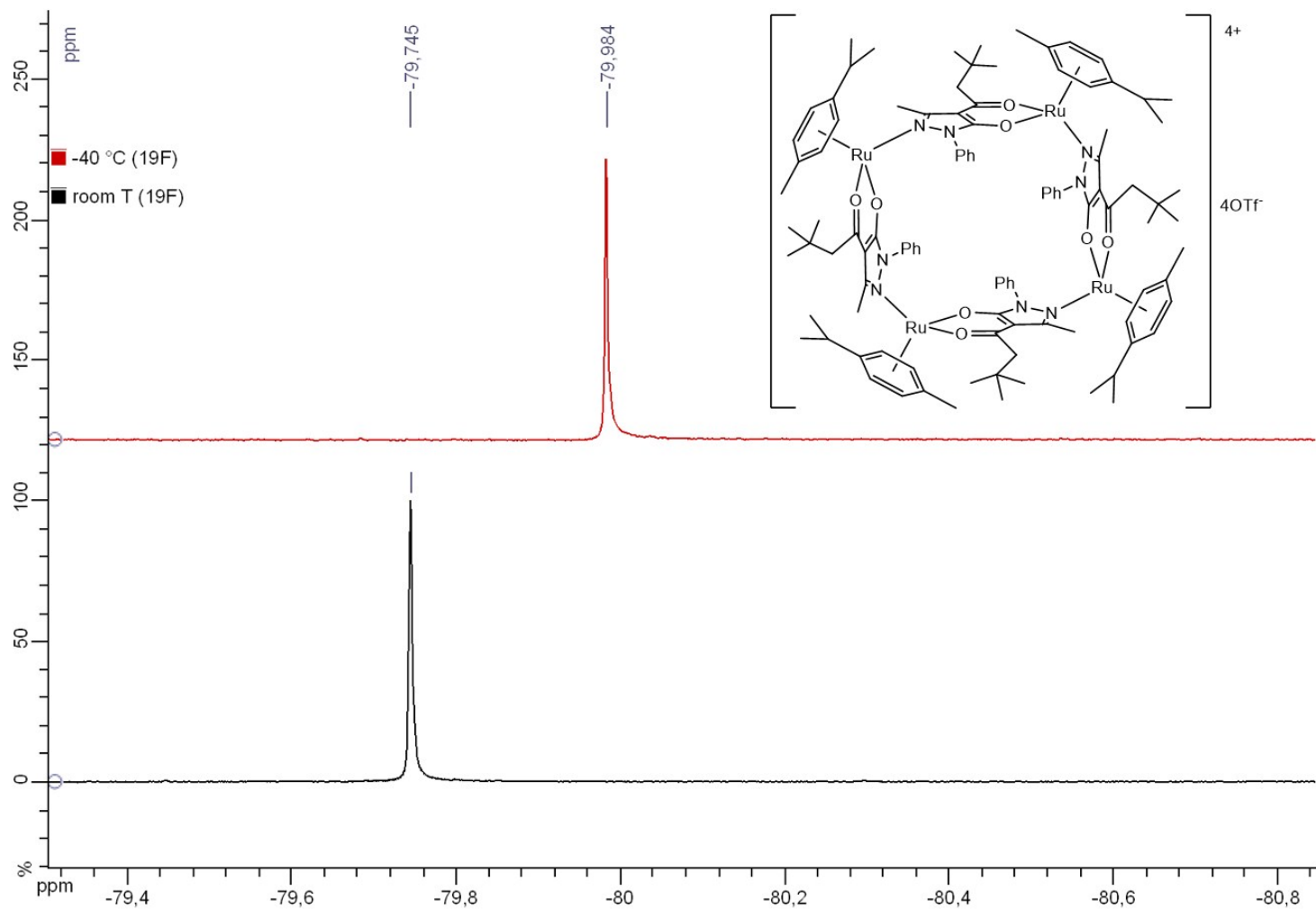


Figure S4. Variable temperature ^{19}F NMR spectra of $[(\eta^6\text{-cym})\text{Ru}(\text{Q}^{\text{nPe}})]_4(\text{SO}_3\text{CF}_3)_4$ (**7**) carried out in CD_3CN .

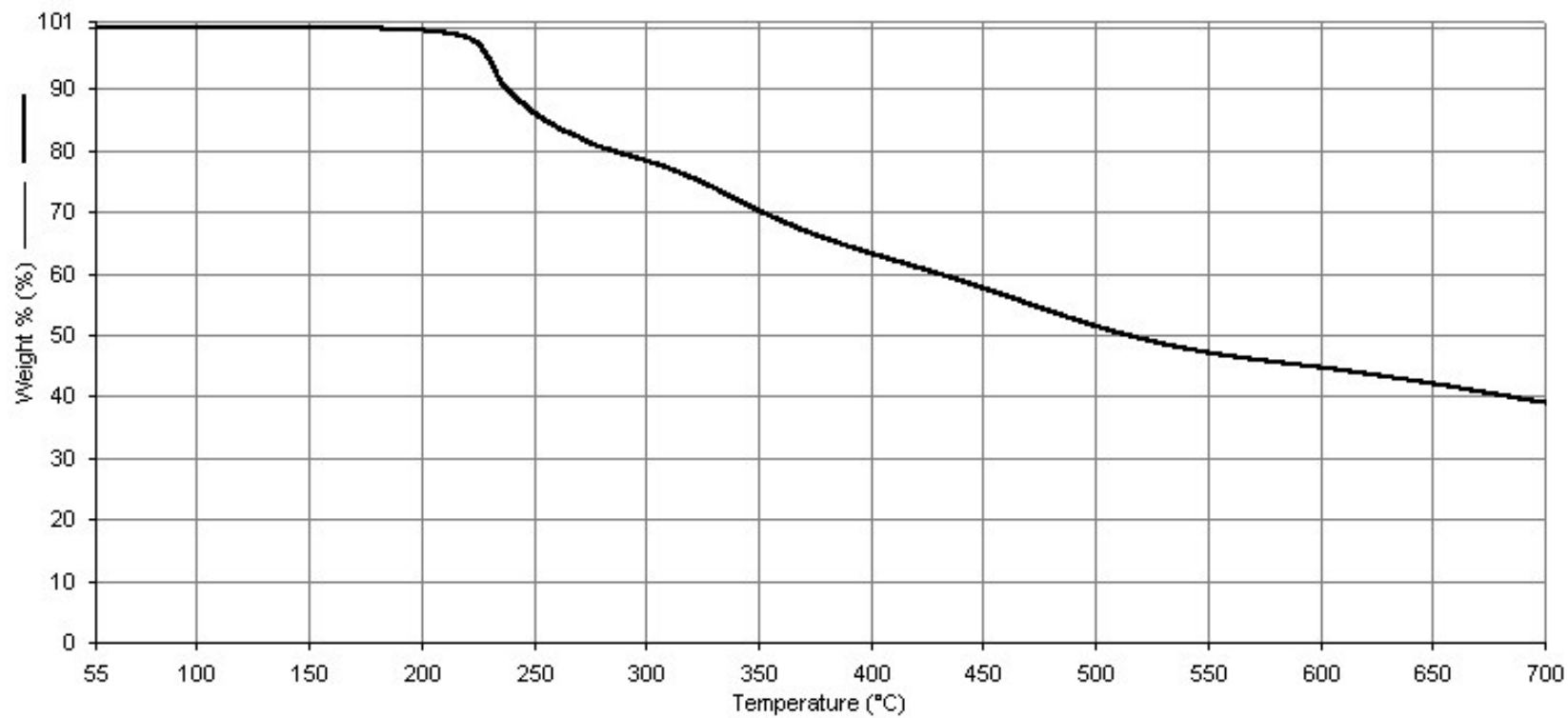


Figure S5. TGA of ligand HQ^{CH2Cl}.

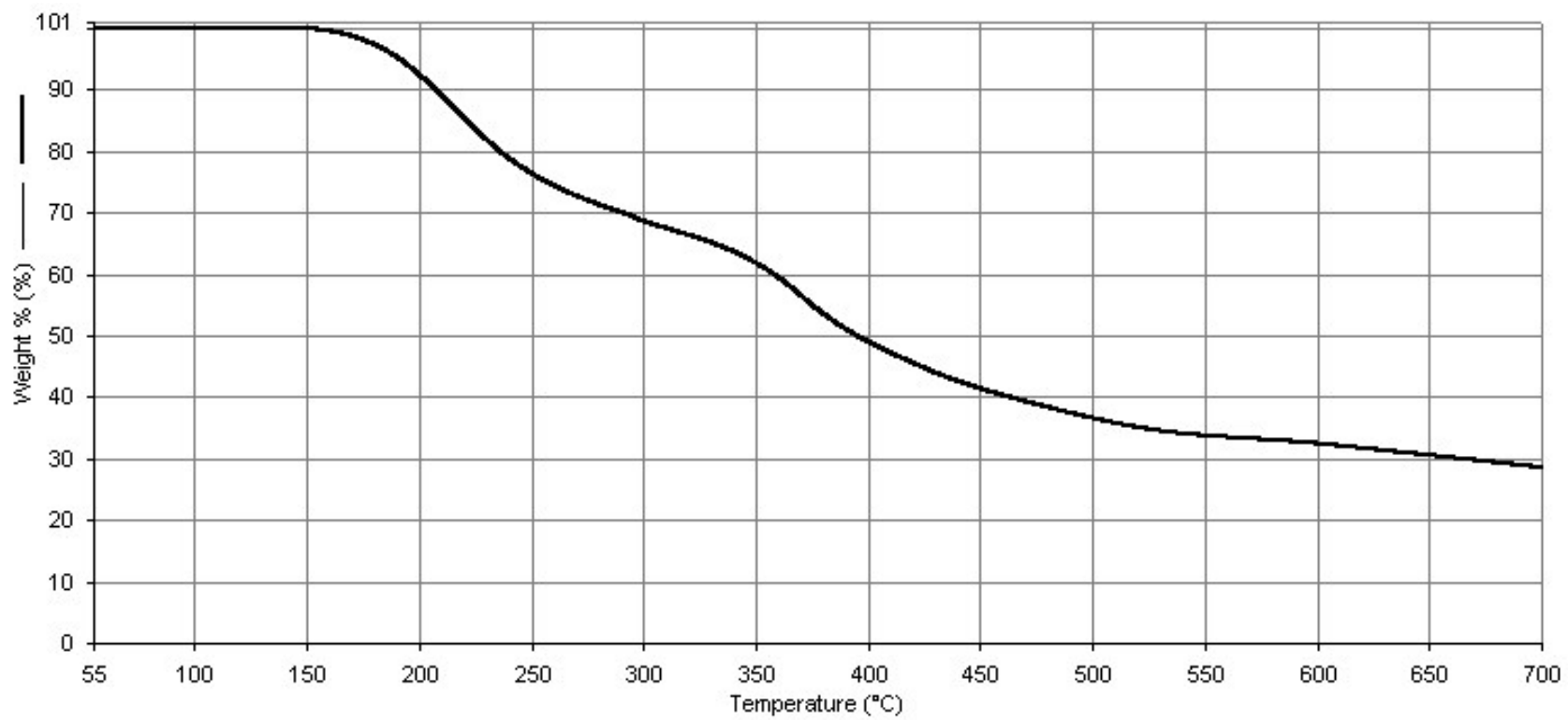


Figure S6. TGA of ligand HQ^{hex}.

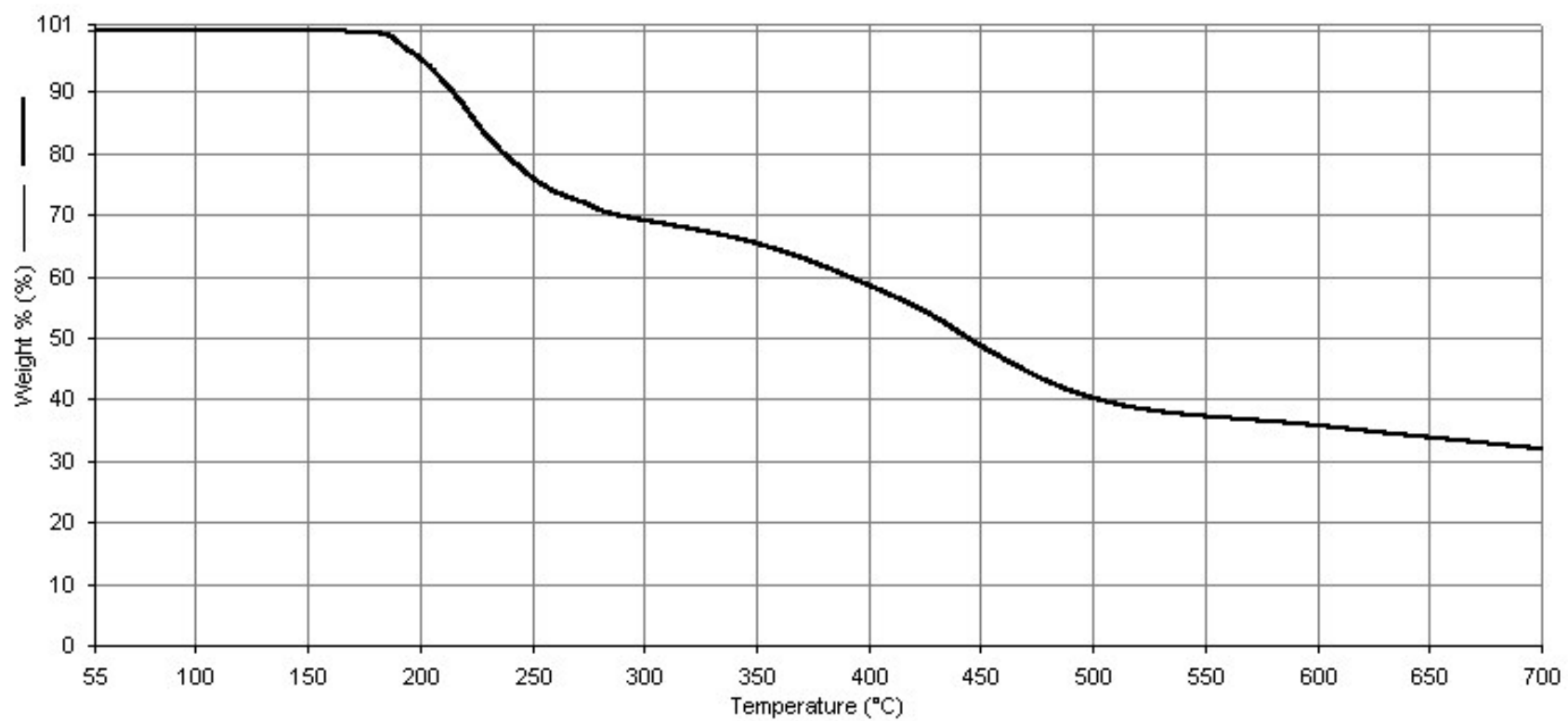


Figure S7. TGA of ligand HQ^{Pe}.



Figure S8. TGA of $[(\eta^6\text{-cym})\text{Ru}(\text{Q}^{\text{CH}_2\text{Cl}})\text{Cl}]$ (**1**).



Figure S9. TGA of $[(\eta^6\text{-cym})\text{Ru}(\text{Q}^{\text{hex}})\text{Cl}]$ (**2**).



Figure S10. TGA of $[(\eta^6\text{-cym})\text{Ru}(\text{Q}^{\text{nPe}})\text{Cl}]$ (**3**).

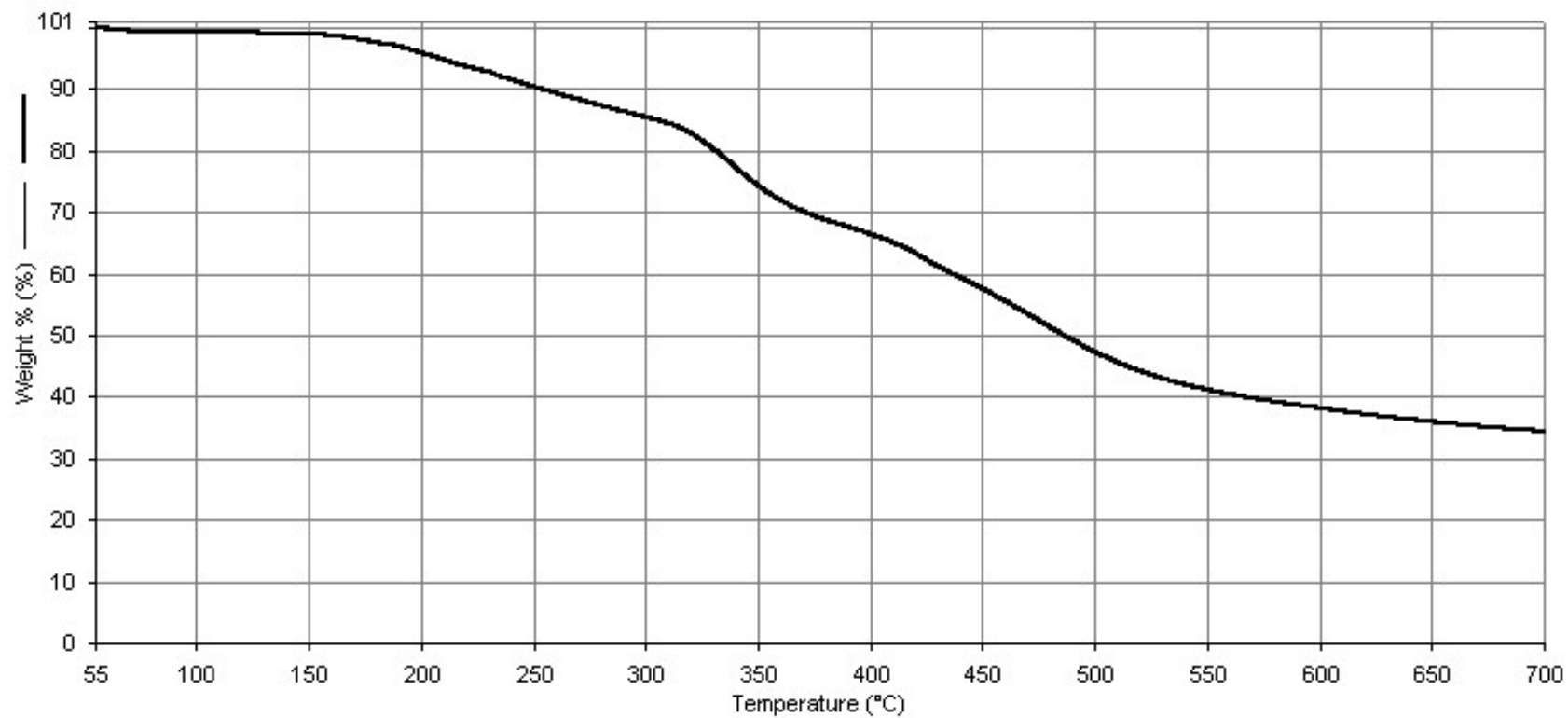


Figure S11. TGA of $\{[(\eta^6\text{-cym})\text{Ru}(\text{Q}^{\text{CH}_2\text{Cl}})]_4(\text{OTf})\}(\text{OTf})_3$ (**4**).

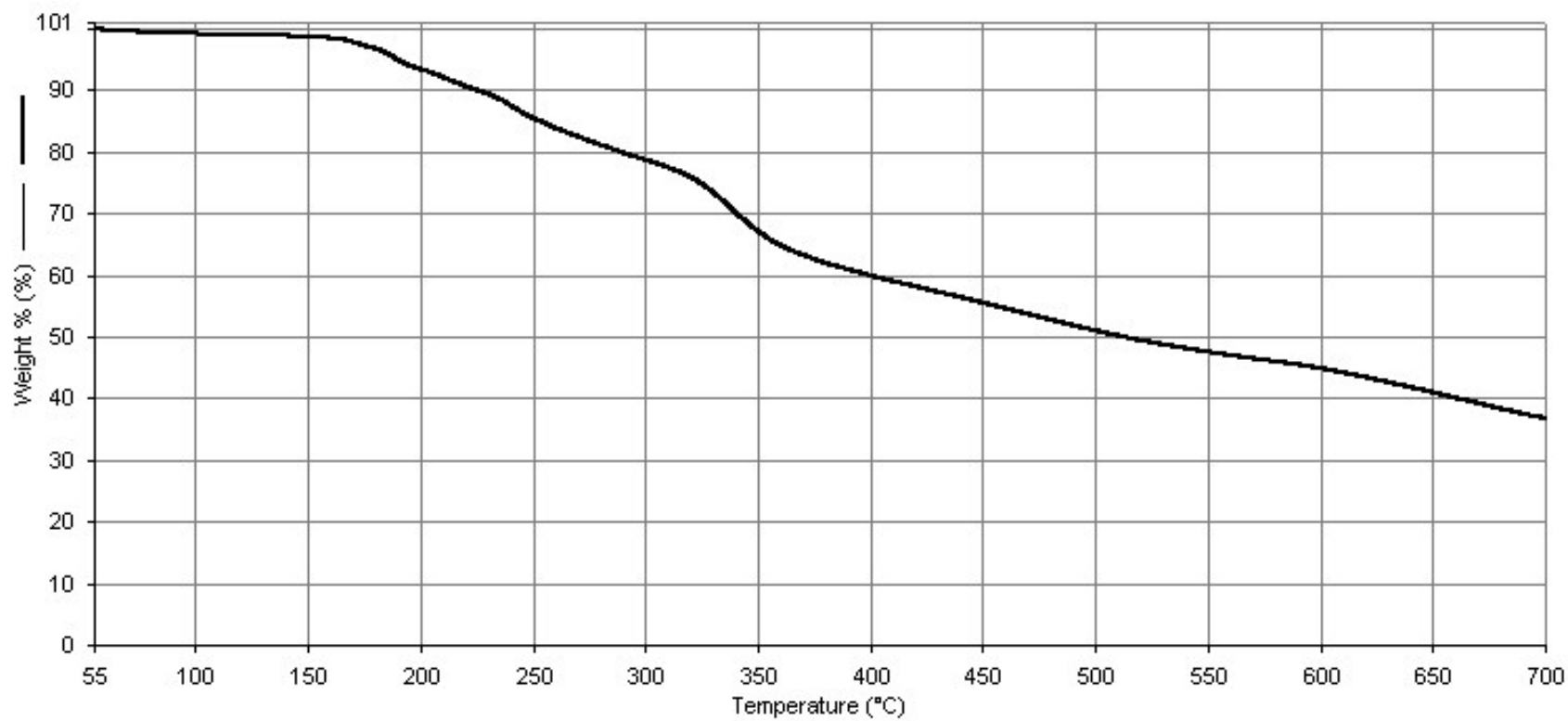


Figure S12. TGA of $\{[(\eta^6\text{-cym})\text{Ru}(\text{Q}^{\text{CH}_2\text{Cl}})]_4(\text{BF}_4)\}(\text{BF}_4)_3$ (**5**).

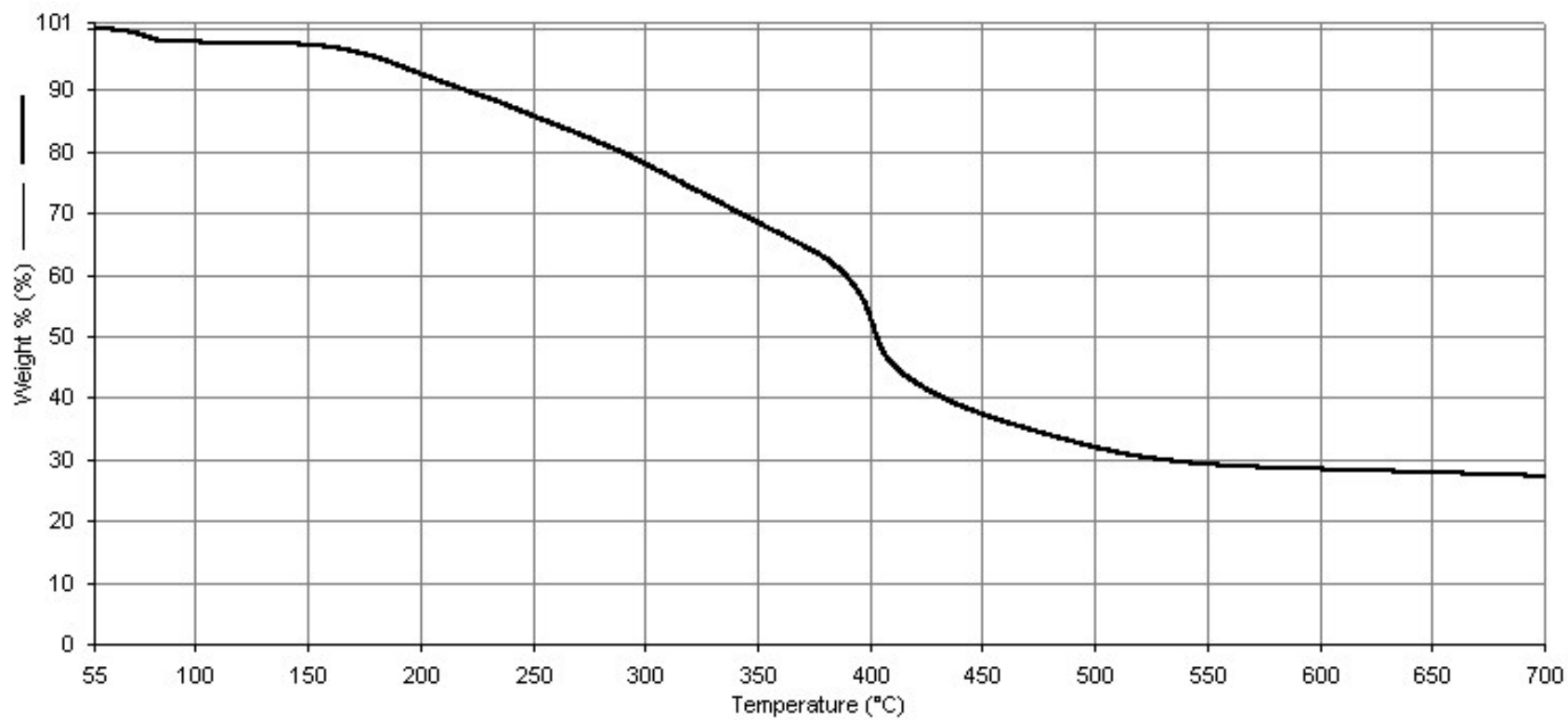


Figure S13. TGA of $\{[(\eta^6\text{-cym})\text{Ru}(\text{Q}^{\text{hex}})]_4(\text{OTf})\}(\text{OTf})_3$ (**6**).

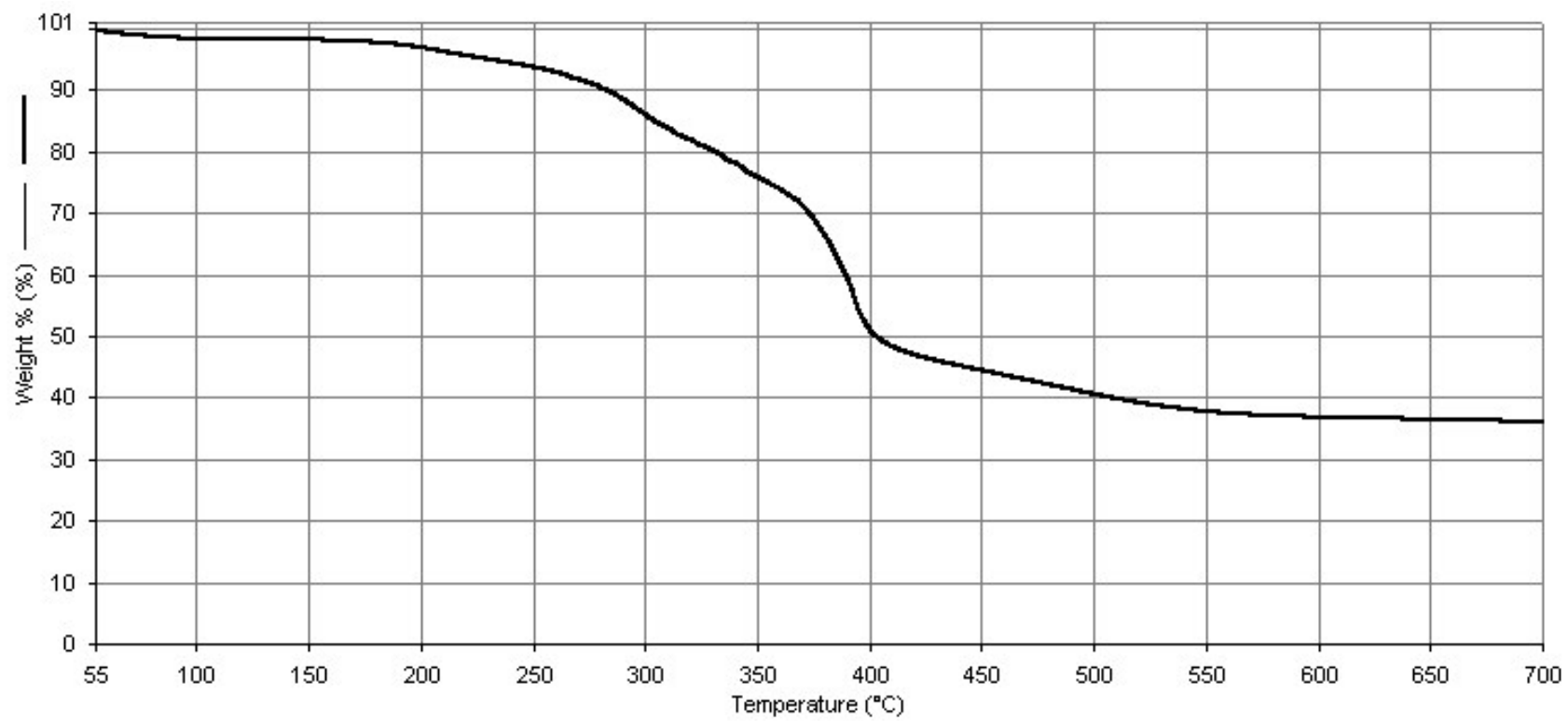


Figure S14. TGA of $\{[(\eta^6\text{-cym})\text{Ru}(\text{Q}^{\text{nPe}})]_4(\text{OTf})\}(\text{OTf})_3$ (**7**).

